THE JOURNAL OF PHYSICAL CHEMISTRY C

ARTICLE

pubs.acs.org/JPCC

DFT Study on Amino-Phospholipids Surface-Mediated Decomposition of Hydrogen Peroxide

Christian Solís-Calero, Joaquín Ortega-Castro, and Francisco Muñoz*

Institut d'Investigació en Ciències de la Salut (IUNICS), Departament de Química, Universitat de les Illes Balears, E-07122 Palma de Mallorca, Spain

ABSTRACT: Hydrogen peroxide molecules play a significant role in controlling certain cellular functions, and its excess causes significant damage to biological systems. There is experimental evidence that its decomposition is accelerated above phospholipids membranes surface. We propose a mechanism for decomposition of hydrogen peroxide on amino-phospholipids surface model based in Dmol3/DFT calculations. The model was built using periodic boundary conditions. Each unit cell contained two phospholipids molecules, two hydrogen peroxide molecules, and nine water molecules. In the studied reaction, two hydrogen peroxide molecules react in a bimolecular reaction to yield an oxygen molecule and two waters. The reaction proceeds by two steps. In the first step, an intermediate hydrogen trioxide from two H_2O_2 molecules is formed. In the second step, this intermediate is cleaved in O_2 and H_2O. There are proton exchanges along the interface between water and amine-phospholipids monolayer in all parts of the pathway. A parallel periodic model of pure water was built to compare the free energy variation through the reaction. Our results show that first step, intermediate hydrogen trioxide formation, is the limiting step of the reaction, having a free energy barrier of 8.76 kcal mol^{-1} in the amino-phospholipids surface model and 25.56 kcal mol^{-1} in the case of pure water model. It could be hypothesized that cell membrane surface environment could enhance this reaction by a neighboring catalyst effect.

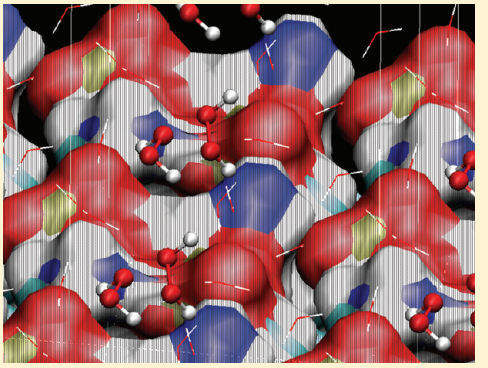

INTRODUCTION

Hydrogen peroxide (H_2O_2) is considered to be an intermediate molecule in several biochemical redox reactions.[1−4] It is usually produced mainly from dismutation of superoxide by superoxide dismutase enzyme and also formed by some oxidases enzymes, such as glucose oxidase or xanthine oxidase. Mitochondria constantly generate small amounts of superoxide, which is rapidly converted to hydrogen peroxide (H_2O_2), which escapes from the mitochondria into the cytosol and modulates cytosolic redox state.[5] In the presence of transition metals (e.g., Fe^{2+}), H_2O_2 may react in a Fenton reaction forming the reactive hydroxyl radical.[6,7]

Biologically, H_2O_2 is essential for functions related to signal transduction, cell growth enhancement, cell proliferation, cell differentiation, and apoptosis.[8−11] In the brain, H_2O_2 has been shown to have several signaling roles,[12−18] contributing to the adjustment of brain function to cellular metabolism and metabolic supply.[19] H_2O_2 may be produced in excess in pathological events, affecting neural cells.[20−24] H_2O_2 is also an inactivating agent of some metalloproteins[25] and, being easily converted to hydroxyl radical, indirectly could cause damage to many cellular components or even cell death.[26]

This dual and contradictory potential of H_2O_2 could be explained as a consequence of its physicochemical properties. It could be a signaling agent because of its membrane permeability and relative inertia,[27] in contrast with other reactive oxygen species (ROS) like superoxide ($O^{2-\bullet}$) or the hydroxyl radical ($OH^{\bullet}$).[28] However, it could cause biological damage because it is capable of oxidizing a wide range of substrates.[29] This raises the question of what biochemical mechanisms could be used to be sufficiently permissive to allow messages to be conveyed and at the same time provide adequate protection against oxidative damage. The defense against H_2O_2 is achieved by natural antioxidant molecules as ascorbate[30,31] and also by antioxidant enzymes; H_2O_2 is degradated by catalase and glutathione peroxidase, which could act cooperativitily.[32,22] However, it is possible to speculate about the existence of another additional intrinsic biochemical mechanisms that limit the toxic effects of H_2O_2.

The cell membrane surface is a special environment, and it can indeed interact with various molecules, including not only small molecules[33−36] but also macromolecules,[37−39] via electrostatic and hydrophobic interactions, hydrogen bonding, or both. The cell membrane surface could also influence the speed of some reactions through a neighboring catalyst effect. It has been showed experimentally in the case of nonenzymatic glycation of phospholipids, whose kinetics is faster than that of protein glycation,[40] and computationally in the case of Schiff base formation.[41] There is experimental evidence that decomposition H_2O_2 could be accelerated above phospholipids membranes surface.[42,43]

Received: July 7, 2011
Revised: October 5, 2011
Published: October 14, 2011

dx.doi.org/10.1021/jp2064134 | J. Phys. Chem. C 2011, 115, 22945–22953

Scheme 1. Mechanism of Hydrogen Peroxide Decomposition on an Aminophospholipid Surface Using Periodic Boundary Conditions[a]

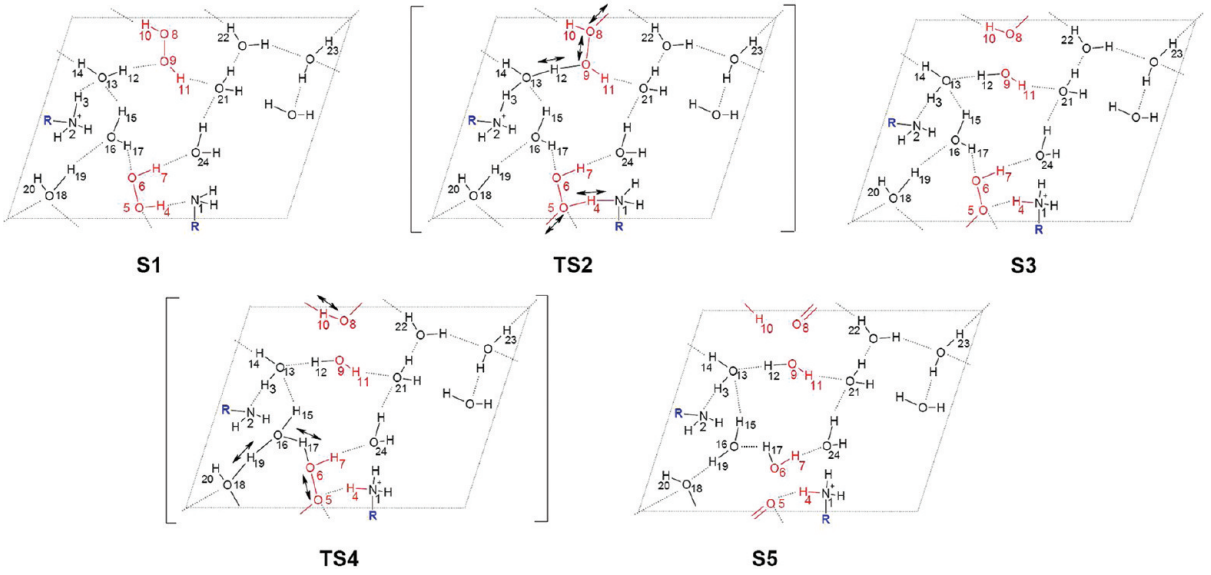

[a] Dotted lines represent hydrogen bonds.

The process of H_2O_2 decomposition into water and oxygen in aqueous solution is thermodynamically favorable. However, the decomposition rate at room temperature is immeasurably small. The rate can be appreciably increased by the addition of a catalyst, which could be homogeneous as Fe^{3+} ions or heterogeneous as manganese dioxide, silver, and platinum.[44−48] In the presence of certain catalysts, such as Fe^{2+} or Ti^{3+}, the H_2O_2 decomposition involves a free radical mechanism, being formed free radicals such as HO and HOO. In vivo the H_2O_2 decomposition is catalyzed by a whole battery of enzymes: catalases, catalase-peroxidases, peroxidases, and peroxiredoxins. In the three first cases, it is through an heterolytic cleavage of the peroxidic bond; H_2O_2 reacts with ferric states of heme-containing enzymes in a two-electron redox reaction.[49] In the case of peroxiredoxins, a cysteinyl residue reacts with the H_2O_2 as primary catalytic center and oxidizes to sulfenic acid.[50,51]

Computationally, H_2O_2 has been studied as a reactive oxygen specie in several organic and inorganic reactions[52−55] and as product or substrate of enzymatic reactions.[56−61] Its adsorption and dissociation on Fe-filled single-walled carbon nanotubes,[62] on Pt and Pt−Alloy clusters and surfaces,[63] and its conformational properties[64] have been also studied theoretically. There are few studies about reactivity on the phospholipid membrane surface. It has been previously reported that the interfacial region of the cell membrane could interact with several small molecules[65,66,36] via electrostatic and hydrophobic interactions, hydrogen bonding, or both. The cell membrane surface could also enhance the ability of protons to diffuse promptly along the membrane through hydrogen-bonded networks of water molecules and charged or polar groups of phospholipids at the surface.[67] The membrane-buried layers of these networks can eventually serve as a storage/buffer for protons (proton sponges).[68,69] The reactivity of phospholipid components of cell membrane has been shown; examples of such reactions are the reactivity of Cl_2 and HOCl by phosphatidylethanolamine,[70] changes due to oxidative stress,[71] and formation of Schiff bases with ketonic compounds.[41,40,72]

In the present Article, we developed a theoretical mechanism for this reaction on amino-phospholipids surface based on hypothesized mechanism of H_2O_2 decomposition, mediated by phospholipids vesicles,[42] and considering the proton conduction through a hydrogen bond network on aminophospholipids surface.[41,73,74] This reaction has been also considered as a model for the investigation of reactivity at phospholipids surfaces, allowing us to analyze the role of head phospholipids functional groups and solvation waters and helping us to understand other reactions on the amino-phospholipids surface.

METHODOLOGY

The amino-phospholipids surface model was represented using a three-dimensionally periodic slab model. The supercell (Figure 1A) contained two molecules of truncated phosphatidylethanolamine, two molecules of hydrogen peroxide, and nine water molecules as explicit solvent in a hydrogen-bond network along the polar heads of phospholipids and was separated from its periodic image by 15 Å of vacuum. They were chosen as the model compound to study the hydrogen peroxide decomposition on the amino-phospholipids surface. One of the phosphatidylethanolamine molecules had a neutral amine group, and the other had a charged amine group to assist the first step of studied reaction acting as proton donor and acceptor. The included nine water molecules cover as a fully connected hydrogen bond network monolayer above the aminophospholipid surface the area of 77 $Å^2$ imposed by the periodic slab dimensions. They satisfied at the same time the specific interactions of the hydrogen bonds between solvent and functional groups of aminophospholipid heads, observed in other studies,[75,76] and the interactions directly involved in proton transfer processes, during the reaction. Probed fewer number of water molecules did not satisfy these conditions. An additional solvent environment was modeled via the conductor-like screening model (COSMO).[77−79] Another periodic system for studying the reaction in pure water was modeled at the same time; this model included 2 molecules

Scheme 2. Mechanism of Hydrogen Peroxide Decomposition in a Pure Water Model Using Periodic Boundary Conditions[a]

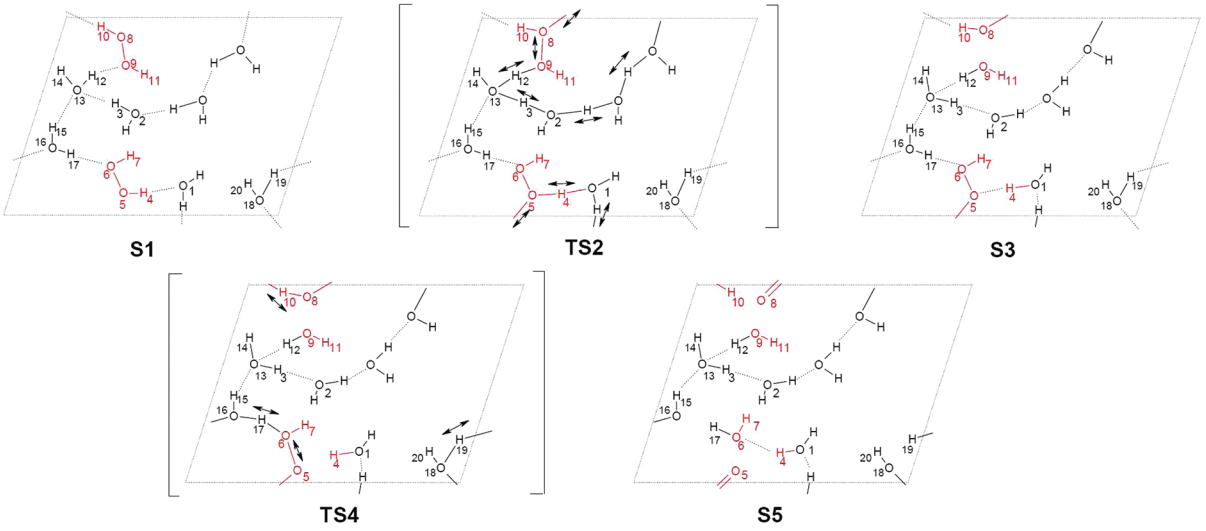

[a] Dotted lines represent hydrogen bonds.

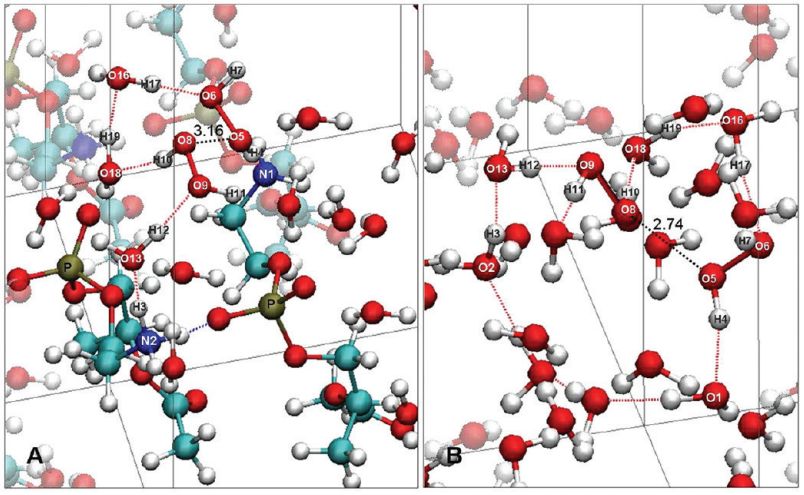

Figure 1. Section of unit cells for the initial studied models. (A) Model of amino-phospholipids surface with two phosphatidylethanolamine, two hydrogen peroxide molecules, and the water hydrogen-bond network by cell. (B) Model of pure water with two hydrogen peroxide molecule, and 17 water molecules by cell. Phosphorus and reactive atoms are labeled and red dotted lines represent hydrogen bonds; in pure water model the number of atoms are labeled according the label of their equivalent atoms in the amino-phospholipids surface model.

of H_2O_2, 17 water molecules by cell, and also the addition of COSMO implicit solvent (Figure 1B); the distribution of H_2O_2 and water molecules in the hydrogen bond network was modeled in a similar way to the amino-phospholipids surface model. The periodic boundary conditions allow the proton transfer across the cells in several steps for the studied reaction in both models (Schemes 1 and 2).

All of the calculations were performed in the frame of DFT with program package DMol3 of Accelrys[80−82] using double numerical with polarization (DNP) basis sets[80] and Perdew−Burke−Ernzerhof (PBE) generalized gradient approximation (GGA) exchange-correlation functional.[83,84] The DNP numerical basis set is comparable to Gaussian 6-31G(d,p),[85−87] minimizes the basis set superposition error,[88] and its accuracy for describing hydrogen-bond strengths has been tested, having obtained a good agreement with experimental values.[89] The maximum number of numerical integration mesh points available in DMol3 was chosen for our computations; the threshold of density matrix convergence was set to 10^{-6}. A Fermi smearing of 0.005 hartree and a real-space cutoff of 4.5 Å were also used to improve the computational performance.

The initial models as reactants and the next models for stationary points generated during H_2O_2 decomposition were modeled in Materials Visualizer, and optimized using the conjugated gradient algorithm. Transition state (TS) searches were performed with the complete LST/QST method.[90] In this method, the linear synchronous transit (LST) maximization was performed, followed by an energy minimization in directions conjugating to the reaction pathway to obtain approximated TS. The approximated TS was used to perform quadratic synchronous

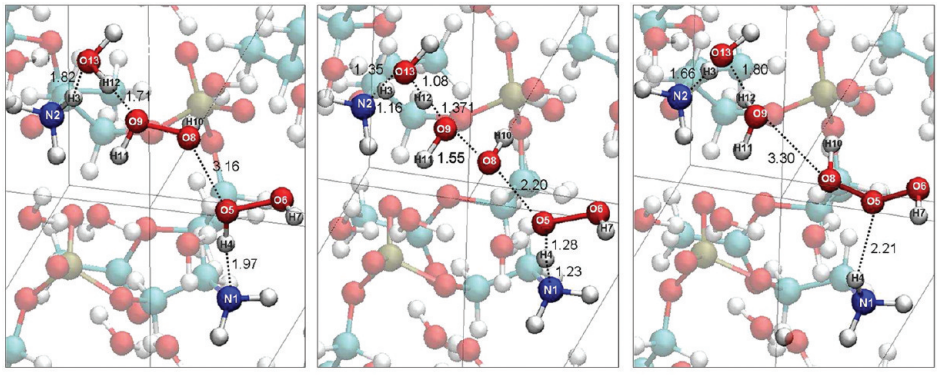

Figure 2. Pathway for hydrogen trioxide formation. (a) Two hydrogen peroxide molecules (S1); (b) transition state (TS2); and (c) hydrogen trioxide product (S3).

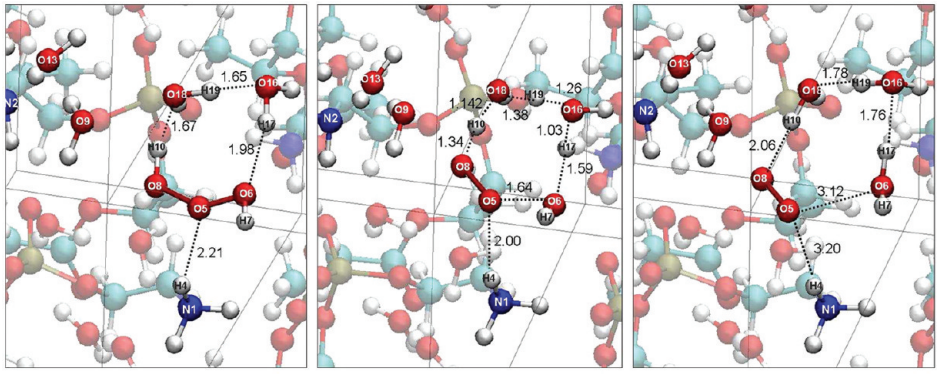

Figure 3. Pathway for O_2 and H_2O formation. (a) Hydrogen trioxide (S3); (b) transition state (TS4); and (c) O_2 and H_2O products (S5).

Table 1. Relative Energies and Free Energies for the Structures of the Studied Reaction Paths

	on aminophospholipid surface		in pure water	
structure	ΔE (kcal mol^{-1})	ΔG (kcal mol^{-1})	ΔE (kcal mol^{-1})	ΔG (kcal mol^{-1})
S01	0.00	0.00	0.00	0.00
TS02	13.04	8.76	30.72	25.56
S03	−8.60	−8.85	−12.62	−15.97
TS04	−1.82	−5.98	−2.65	−13.97
S05	−21.37	−24.17	−30.37	−35.27

transit (QST) maximization, and then another conjugated gradient minimization was performed. The cycle was repeated until a stationary point was located. The obtained TS was optimized via eigenvector following, searching for an energy maximum along one previous selected normal mode and a minimum along all other nodes, using Newton−Raphson method. After this procedure, one transition state was found for each reaction step. Each TS structure was characterized by a vibrational analysis with exactly one imaginary frequency. Mulliken population analysis was used to understand the charge flow on-group migration.

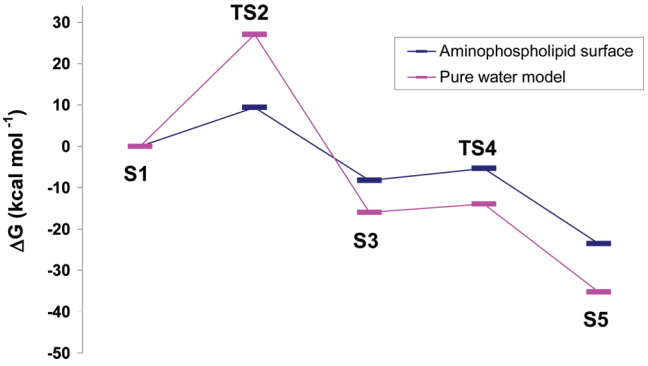

Figure 4. Free-energy profiles for the reaction on amino-phospholipids surface and pure water models.

RESULTS AND DISCUSSION

The structures found allow the outline of detailed chemical paths for the decomposition of hydrogen peroxide on amino-phospholipids surface and in pure water models. Atoms directly related to reaction and the completely process are shown in Figures 2 and 3 and Schemes 1 and 2. It can be described by means of two main steps: formation of intermediate hydrogen trioxide (Figure 2) and its decomposition in O_2 and H_2O

dx.doi.org/10.1021/jp2064134 |J. Phys. Chem. C 2011, 115, 22945–22953

Table 2. Some Geometric Parameters of Structures Presented in Scheme 1[a]

structures		S1	TS2	S3	TS4	S5
distances	N1−H4	1.972	1.233	1.031	1.034	1.051
	H4−O5	1.005	1.284	2.207	2.002	3.196
	O5−O6	1.469	1.477	1.466	1.644	3.117
	O6−H7	1.012	0.998	1.009	0.997	0.988
	O5−O8	3.159	2.205	1.439	1.36	0.980
	O8−H10	0.996	1.007	1.018	1.336	2.055
	O8−O9	1.469	1.554	3.301	3.245	3.690
	O9−H12	1.707	1.371	0.991	0.984	0.988
	H12−O13	0.999	1.079	1.803	1.924	1.856
	O13−H3	1.818	1.347	1.036	1.068	1.027
	H3−N2	1.050	1.161	1.659	1.564	1.699
	H10−O18	1.823	1.738	1.670	1.142	0.980
	O18−H19	1.008	1.008	1.013	1.377	1.781
	H19−O16	1.654	1.667	1.637	1.104	0.992
	O16−H17	0.991	1.001	0.983	1.029	1.755
	H17−O6	1.832	1.74	1.977	1.587	0.999
	O16−H15	0.996	0.991	1.010	1.078	0.996
	H15−O13	1.768	1.831	1.648	1.424	1.765
	O5−H22	1.827	1.681	3.389	4.165	4.401
	O8−H22	3.433	2.41	3.299	4.228	5.578
	O18−H23	1.695	1.731	1.656	1.660	1.720
	O9−H11	1.017	1.014	0.985	0.986	0.985
	H11−O21	1.618	1.676	1.885	1.892	1.906
angles	O6−O5−O8	94.2	119.4	109.2	112.3	109.4
	O5−O8−O9	111.9	167.7	160.5	156.4	55.9
dihedral angles	H7−O6−O5−H4	−94.0	−99.5	−48.5	−68.9	124.2
	H10−O8−O9−H11	94.0	150.9	152.4	166.4	−160.4

[a] Distances in angstroms and bond and dihedral angles in degrees

(Figure 3). Table 1 shows relative energies and ΔG at 298.15 K and 1 atm for each structure involved in the process. The free-energy profiles for both models appear in Figure 4. Structural-relevant data for each intermediate and transition state are shown in Table 2.

A. Hydrogen Trioxide Formation. In this step (Scheme 1), the dissociation of hydrogen peroxide (H_2O_2) proceeds concertedly through a nucleophilic attack of a first H_2O_2 molecule on the oxygen atom of another H_2O_2 and an hydrolytic cleavage of the O−O bond from the last H_2O_2, forming a dihydrogen trioxide (HOOOH) and water molecules. The pathway of this step could be followed through the variation of the atoms distances N1−H4, H4−O5, O5−O8, O8−O9, O9−H12, H12−O13, O13−H3, and H3−N2 in the structures S1, TS2, and S3 (Table 1).

H_2O_2 is an acid and it could dissociate to hydrogen peroxide anion (HOO^-), which is a strong α-nucleophile.[91,92] Nucleophilic attack of HOO^- has been seen in diverse kinds of systems.[93,94] It has been shown that formation of HOO^- anion is favored by alkaline media.[95,96] In the aminophospholipid surface, a local alkaline environment could be created due to the presence of phosphate groups and nonprotonated amine groups, something that is not possible in neutral water solution. We could not find HOO^- chemical species as a stationary point in our calculus.

The nucleophilic attack polarizes and stretches the O8−O9 bond of the second H_2O_2, breaking this bond hydrolytically, formatting a hydrogen trioxide intermediate and a water molecule. The deprotonation of the first H_2O_2 molecule is done having an amine group (N1) of a phosphatidylethanolamine molecule like a proton acceptor. Concertedly, the charged amine group of another phospholipid acts like proton donor in the hydrolytic cleavage of the second H_2O_2 with the formation of a water molecule: H12O9H11 (Figure 2 and Scheme 1).

For comparative effects, to evaluate the influence of amino-phospholipid surface above the reaction in comparison with an environment of only water explicit solvent, we developed a periodic model for studying the reaction in pure water and the distribution of H_2O_2 and water molecules in the hydrogen bond network, and the addition of COSMO implicit solvent was modeled in a similar way to the amino-phospholipids surface model (Scheme 2).

The first step of this reaction on the amino-phospholipids surface had an energy barrier of 8.76 kcal mol^{-1}, and in the case of pure water model, this energy barrier is 25.56 kcal mol^{-1} (Figure 4 and Table 2). The difference between these values could be explained due to the different environments. In the case of pure water model, there is the absence of charged and neutral amine groups to function as proton donor and acceptor, and, in consequence, the proton transfer is direct between both H_2O_2 molecules, with the assistance of five water molecules. The amino-phospholipids surface environment could also influence in the polarization of reactive H_2O_2 molecules and water molecules, which participate as bridges in the proton exchange between donor and acceptor protons in this reaction step. The polarization effect of aminophospholipid surface was evidenced

Table 3. Mulliken Population Analysis Results for Structures for the Structures of the Studied Reaction Paths in Aminophospholipid Surface (AS) and Pure Water (PW) Models

	S1		TS2		S3		TS4		S5	
atoms	AS	PW	AS	PW	AS	PW	AS	PW	AS	PW
N1[a]	−0.591	−0.596	−0.531	−0.540	−0.392	−0.557	−0.394	−0.57	−0.424	−0.605
N2[a]	−0.419	−0.641	−0.517	−0.746	−0.614	−0.636	−0.612	−0.646	−0.592	−0.656
H3	0.318	0.326	0.394	0.362	0.361	0.316	0.384	0.314	0.366	0.318
H4	0.344	0.324	0.404	0.381	0.3	0.331	0.295	0.332	0.335	0.361
O5	−0.373	−0.329	−0.497	−0.326	−0.151	−0.122	−0.164	−0.104	−0.034	−0.006
O6	−0.402	−0.395	−0.408	−0.387	−0.349	−0.376	−0.463	−0.554	−0.665	−0.664
H7	0.354	0.354	0.337	0.376	0.344	0.362	0.338	0.318	0.307	0.326
O8	−0.364	−0.344	−0.347	−0.356	−0.314	−0.281	−0.396	−0.206	−0.076	−0.03
O9	−0.426	−0.437	−0.456	−0.542	−0.698	−0.657	−0.682	−0.657	−0.679	−0.643
H10	0.342	0.322	0.35	0.338	0.347	0.337	0.388	0.377	0.331	0.292
H11	0.371	0.377	0.365	0.346	0.307	0.3	0.305	0.305	0.301	0.304
H12	0.352	0.335	0.408	0.400	0.311	0.309	0.312	0.3	0.314	0.298
O13	−0.695	−0.653	−0.743	−0.686	−0.737	−0.643	−0.734	−0.642	−0.711	−0.644
O16	−0.667	−0.645	−0.681	−0.629	−0.667	−0.637	−0.592	−0.724	−0.685	−0.654
H17	0.327	0.311	0.332	0.309	0.304	0.304	0.346	0.397	0.312	0.335
O18	−0.702	−0.645	−0.712	−0.621	−0.717	−0.656	−0.795	−0.668	−0.689	−0.623
H19	0.34	0.316	0.341	0.307	0.348	0.319	0.395	0.408	0.322	0.323

[a] In PW model the atoms are labeled according the label of their equivalent atoms in the AS model; N1 and N2 refer to oxygen atoms O1 and O2 with an equivalent role to nitrogen atoms in the mechanism of reaction.

through Mulliken population analysis of S1 structure, where the difference between partial atomic charges of N2 and O13 atoms, proton donor, and acceptor during the hydrolytic cleavage of the O8−O9 bond in the aminophospholipid surface model is clearly greater than the difference between O2 and O13, their equivalent atoms in pure water model (0.275 versus 0.012, Table 3). Proton conduction is also known to be facilitated along phospholipid monolayers spread on aqueous phases;[73] surface charges should modulate such conduction by changing the electrical properties of the interface and, as shown by NMR studies, the local conformations of the polar head regions.[97]

The role of components of aminophospholipid surface is not only limited to participating in proton transfer but also favoring accumulation of the main reactive H_2O_2 on the proximity of the surface. We found the phosphate anion of phospholipids forms hydrogen bonds with water molecules in the network connecting donor and acceptor protons (Figure 1); it could facilitate accumulation of H_2O on the membrane surface and in consequence of H_2O_2 in its proximity, raising local concentrations of the last as a result. Other studies have shown that negatively charged phosphate groups are tightly solvated by an average of four water molecules each[98] and they are also able to support proton conduction.[73]

The existence of the intermediate dihydrogen trioxide (HOOOH) generated in this step has been verified in several studies.[99−102] It has been demonstrated that this trioxide, its radical $HOOO^{\bullet}$, and its anion $HOOO^{-}$ are most likely key intermediates involved in oxidation processes that span atmospheric,[103−105] environmental,[106] and biological systems.[107,108] It has given IR and Raman spectroscopic evidence of the involvement of HOOOH in electrically dissociated mixture of water, hydrogen peroxide, and oxygen,[109,110] and it has been also observed during the thermal reaction between hydrogen peroxide and ozone.[101] Surprising evidence even indicates that HOOOH is also formed as an intermediate in H_2O_2 and ozone production from water and singlet oxygen by antibodies.[108,111,112]

B. Formation of O_2 and H_2O. The next step of the reaction was the decomposition of the intermediate dihydrogen trioxide, with the consequent formation of O_2 and H_2O. In the developed mechanism, it required the assistance of three water molecules around as proton donors and acceptors. These water molecules are connected between them and the intermediate HOOOH through hydrogen bonds. The pathway of this step could be followed through the variation of the atoms distances O6−O5, O5−O8, O8−H10, H10−O18, O18−H19, H19−O16, O16−H17, and H17−O6 in the structures S3, TS4, and S5 (Table 1). In a concerted way, there is a proton transfer from O8 atom of HOOOH to O6 of the same molecule (Figure 3), having three water molecules like a bridge that make possible it through a Grotthuss mechanism for proton transfer.[113] Concertedly, the O5−O6 bond is considerably polarized, breaking this and leading to the O_2 and H_2O formation. This type of decomposition for HOOOH, facilitated by a Brönsted acid catalysis with the assistance of water molecules, has been suspected by other authors.[114]

There are not great differences between the amino-phospholipids surface and pure water models for the free-energy barriers for this reaction step. In the first case, the free-energy barrier had a value of 2.86 kcal mol^{-1} and in the case of pure water model a value of 2.00 kcal mol^{-1} (Figure 4 and Table 2). It could be due to the less influence of the aminophospholipid surface on the polarization of the atoms involved in the reaction. Mulliken population analysis of S3 structure (Table 3) has shown that the difference between partial Mulliken atomic charges of the couples of proton donors and acceptors in this step (O16 and O6 in AS model, 0.318, and O8 and O18 in PW model, 0.375) is smaller than in the first step.

A theoretical study about intramolecular 1,3-proton transfer in HOOOH to give H_2O and O_2, using MP4//MP2/6-31++G(d) level of calculus on gas phase,[115] considered also the participation

dx.doi.org/10.1021/jp2064134 |J. Phys. Chem. C 2011, 115, 22945–22953

of H_2O in the reaction as a catalyst. They followed several possible decomposition paths, finding an energy barrier of 48.6 kcal mol^{-1} for the unassisted intramolecular proton transfer (only HOOOH) and a barrier of 26 kcal mol^{-1} for the water-assisted intermolecular reaction (HOOOH-H_2O complex). Another study at B3LYP/6-31G** level[116] for the same reaction indicated that the unimolecular decomposition of HOOOH had a barrier of 44.9 kcal mol^{-1}, whereas the water-catalyzed decomposition of HOOOH had a barrier of 20.0 kcal mol^{-1} (from the complex), confirming the shown tendency of the another study. The authors were expecting that the energy barrier would be lowered further if more water molecules would participate in the decomposition. This hypothesis has been confirmed in our research, where the involvement of three additional molecules of water, considering both an amino-phospholipids surface and pure water models, lower the total energy barrier of this process to 6.78 and 9.97 kcal mol^{-1}, respectively (ΔE in Table 1).

In the same study,[116] when the inverse reaction, the formation of HOOOH from O_2 and H_2O, was studied, a total energy barrier of 61.1 kcal mol^{-1} was found, explained above all due to the reaction heat of ΔH_r = 46.0 kcal mol^{-1} for hydrogen abstraction to form HO^- and HOO^-; when a water molecule in the system to assist the reaction was considered, this barrier was 33.1 kcal mol^{-1}. In our study, the calculated total energy barrier for this direction of the reaction $O_2 + H_2O \rightarrow$ HOOOH, considering three water molecules to assist the proton transfer, was 19.55 kcal mol^{-1} in the case of amino-phospholipids surface model and 27.72 kcal mol^{-1} in pure water model (Table 1). The reduction of the value in the first case could be explained in part by the influence of the amino-phospholipids surface environment, which would make more favorable the proton abstraction due to the proximity of alkaline phosphate groups, and in both models by the participation of three water molecules that participate as a bridge in the proton transfer between water and oxygen molecules, contributing also to decrease the energy barrier. This direction of the reaction is interesting because there are experimental observations about the formation of HOOOH from H_2O and O_2, catalyzed by antibodies and T cell receptors,[108,112,117,118] being dihydrogen trioxide in this context, a key intermediate to the formation of endogenous ozone in human atherosclerotic arteries.[119]

Other theoretical and experimental investigations have confirmed the catalytic role of water in the polar HOOOH decomposition.[99,120−123] It has been also reported the fast autocatalytic decomposition of HOOOH to produce water and O_2 in nonpolar solvents (toluene) due to the existence of dihydrogen trioxide clusters, $(HOOOH)_n$, but not in organic oxygen base solvents (acetone and dimethyl ether), where the H bonds that stabilize the clusters of HOOOH may be disrupted,[124] something that is also expected in water.

From the reaction profiles (Figure 4), the structure of transition state TS4 should be S3 structure, according to the Hammond postulate, which assumes that the transition states for reactions involving unstable intermediates, in this case, HOOOH molecule, can be closely approximated by the intermediates themselves. That is confirmed from structural data (Table 1) where the distances between reactive atoms (e.g., O5−O6, O5−H4) and parameters like angles and dihedrals are more similar between structures S3 and TS4 than between TS4 and S5 in the aminophospholipid surface model. In the case of S5 structure, it is necessary to consider the oxygen molecule freedom that has highly reduced Mulliken partial charges (Table 3) and thus less strong electrostatic interactions with the molecules around, being able to be stabilized easily in different conformations on the designed molecular system.

C. Conclusions. Our DFT calculations provide strong evidence that the dissociation of hydrogen peroxide on amine-phospholipid surface proceeds in two steps. In the first step, it forms an intermediate hydrogen trioxide from two H_2O_2 molecules; in the second step, this intermediate is cleaved in O_2 and H_2O via concerted mechanisms, being the first step, the limiting step of the reaction. According to the proposed mechanism, the surface membrane, including water molecules of solvation, could mediate decomposition of H_2O_2, lowering the free-energy barrier for the first step of the reaction by a neighboring catalyst effect, acting as proton donor and acceptor during the reaction and polarization of atoms implied in the reaction as a result of an interaction with functional groups of aminophospholipids polar head. Its influence in the accumulation of H_2O_2 on surface could be hypothesized, resulting in increased local concentrations. In the second step of the reaction, water behaves as a bifunctional catalyst (proton and donor−acceptor) and thus participates in a polar (nonradical) decomposition process of the intermediate dihydrogen trioxide.

AUTHOR INFORMATION

Corresponding Author

*Tel: + 34 971 17 32 52. Fax: + 34 971 17 34 26. E-mail: dqufmi0@uib.es.

ACKNOWLEDGMENT

This work was funded by the Spanish Government in the framework of project CTQ2008-02207/BQU. We gratefully acknowledge technical support and extensive discussions with Dr. A. Hernández-Laguna (Estación Experimental del Zaidín, CSIC, Granada). C.S.-C. acknowledges a MAE-AECI fellowship from the Spanish Ministry of Foreign Affairs and Cooperation. We are grateful to Centro de Cálculo de Computación de Galicia (CESGA) and the Centro de Cálculo de Computación de Cataluña (CESCA) for access to their computational facilities.

REFERENCES

(1) Flohé, L. *Methods Enzymol.* **2010**, *473*, 1–39.
(2) Quan, L. J.; Zhang, B.; Shi, W.W-; Li, H. Y. *J. Integr. Plant Biol.* **2008**, *50*, 2–18.
(3) Giorgio, M.; Trinei, M.; Migliaccio, E.; Pelicci, P. G. *Nat. Rev. Mol. Cell Biol.* **2007**, *8*, 722–728.
(4) Noctor, G.; Veljovic-Jovanovic, S.; Foyer, C. H. *Philos. Trans. R. Soc., B* **2000**, *355*, 1465–1475.
(5) Tretter, L.; Takacs, K.; Kövér, K.; Adam-Vizi, V. *J. Neurosci. Res.* **2007**, *85*, 3471–3479.
(6) Jomova, K.; Vondrakova, D.; Lawson, M.; Valko, M. *Mol. Cell. Biochem.* **2010**, *345*, 91–104.
(7) Winterbourn, C. C. *Toxicol. Lett.* **1995**, *82−83*, 969–974.
(8) Forman, H. J. *Ann. N.Y. Acad. Sci.* **2010**, *1203*, 35–44.
(9) Domínguez, L.; Sosa-Peinado, A.; Hansberg, W. *Arch. Biochem. Biophys.* **2010**, *500*, 82–91.
(10) Groeger, G.; Quiney, C.; Cotter, T. G. *Antioxid. Redox Signaling* **2009**, *11*, 2655–2671.
(11) Veal, E. A.; Day, A. M.; Morgan, B. A. *Mol. Cell* **2007**, *26*, 1–14.
(12) Pellmar, T. C. *Neuroscience* **1987**, *23*, 447–456.
(13) Avshalumov, M. V.; Rice, M. E. *J. Neurophysiol.* **2002**, *87*, 2896–2903.
(14) Chen, B. T.; Avshalumov, M. V.; Rice, M. E. *J. Neurophysiol.* **2002**, *87*, 1155–1158.

(15) Auerbach, J. M.; Segal, M. *J. Neurosci.* **1997**, *17*, 8695–8701.
(16) Kamsler, A.; Segal, M. *J. Neurosci.* **2003**, *23*, 269–276.
(17) Atkins, C. M.; Sweatt, J. D. *J. Neurosci.* **1999**, *19*, 7241–7248.
(18) Gerich, F. J.; Funke, F.; Hildebrandt, B.; Fasshauer, M.; Müller, M. *Pfluegers Arch.* **2009**, *458*, 937–952.
(19) Dröge, W. *Physiol. Rev.* **2002**, *82*, 47–95.
(20) Chan, P. H. *Neurochem. Res.* **2004**, *29*, 1943–1949.
(21) Coyle, J. T.; Puttfarcken, P. *Science* **1993**, *262*, 689–695.
(22) Olanow, C. W. *Trends. Neurosci.* **1993**, *16*, 439–444.
(23) Behl, C.; Davis, J. B.; Lesley, R.; Schubert, D. *Cell* **1994**, *77*, 817–827.
(24) Seutin, V.; Scuvée-Moreau., J.; Massotte, L.; Dresse, A. *Brain Res.* **1995**, *683*, 275–278.
(25) Arnao, M. B.; Acosta, M.; del Río, J. A.; Varón, R.; García-Cánovas, F. *Biochim. Biophys. Acta* **1990**, *1041*, 43–47.
(26) Rhee, S. G. *Science* **2006**, *312*, 1882–1883.
(27) Ramasarma, T. *Biochim. Biophys. Acta* **1983**, *694*, 69–93.
(28) Cohen, G. *Ann. N.Y. Acad. Sci.* **1994**, *738*, 8–14.
(29) Watt, B. E.; Proudfoot, A. T.; Vale, J. A. *Toxicol Rev.* **2004**, *23*, 51–57.
(30) Imlay, J. A. *Annu. Rev. Biochem.* **2008**, *77*, 755–776.
(31) Avshalumov, M. V.; MacGregor, D. G.; Sehgal, L. M.; Rice, M. E. *Neuron Glia. Biol.* **2004**, *1*, 365–376.
(32) Baud, O.; Greene, A. E.; Li, J.; Wang, H.; Volpe, J. J.; Rosenberg, P. A. *J. Neurosci.* **2004**, *24*, 1531–1540.
(33) Debnath, A.; Mukherjee, B.; Ayappa, K. G.; Maiti, P. K.; Lin, S. T. *J. Chem. Phys.* **2010**, *133*, 174704.
(34) Lukacova, V.; Peng, M.; Tandlich, R.; Hinderliter, A.; Balaz, S. *Langmuir* **2006**, *22*, 1869–1874.
(35) Tsogas, I.; Tsiourvas, D.; Nounesis, G.; Paleos, C. M. *Langmuir* **2005**, *21*, 5997–6001.
(36) Barry, J. A.; Gawrisch, K. *Biochemistry* **1994**, *33*, 8082–8088.
(37) Ortiz, A.; Aranda, F. J.; Teruel, J. A. *Adv. Exp. Med. Biol.* **2010**, *672*, 42–53.
(38) Da Costa, G.; Mouret, L.; Chevance, S.; Le Rumeur, E.; Bondon, A. *Eur. Biophys. J.* **2007**, *36*, 933–942.
(39) Prenner, E. J.; Lewis, R. N.; McElhaney, R. N. *Biochim. Biophys. Acta* **1999**, *1462*, 201–221.
(40) Levi, V.; Villamil Giraldo, A. M.; Castello, P. R.; Rossi, J. P.; González Flecha, F. L. *Biochem. J.* **2008**, *416*, 145–152.
(41) Solís-Calero, C.; Ortega-Castro, J.; Muñoz, F. *J. Phys. Chem. B.* **2010**, *114*, 15879–15885.
(42) Yoshimoto, M.; Miyazaki, Y.; Umemoto, A.; Walde, P.; Kuboi, R.; Nakao, K. *Langmuir.* **2007**, *23*, 9416–9422.
(43) Yoshimoto, M.; Miyazaki, Y.; Sato, M.; Fukunaga, K.; Kuboi, R.; Nakao, K. *Bioconjugate Chem.* **2004**, *15*, 1055–1061.
(44) Kicela, A.; Daniele, S. *Talanta* **2006**, *68*, 1632–1639.
(45) Welch, C. M.; Banks, C. E.; Simm, A. O.; Compton, R. G. *Anal. Bioanal. Chem.* **2005**, *382*, 12–21.
(46) Colodette, J. L.; Rothenberg, S.; Dence, C. W. *J. Pulp. Paper. Sci.* **1988**, *14*, J126–132.
(47) Kiba, N.; Shimizu, K.; Furusawa, M. *Talanta.* **1983**, *30*, 969–970.
(48) Broughton, D. B.; Wentworth, R. L.; Laing, M. E. *J. Am. Chem. Soc.* **1947**, *69*, 744–747.
(49) Vlasits, J.; Jakopitsch, C.; Bernroitner, M.; Zamocky, M.; Furtmüller, P. G.; Obinger, C. *Arch. Biochem. Biophys.* **2010**, *500*, 74–81.
(50) Tavender, T. J.; Bulleid, N. J. *J. Cell. Sci.* **2010**, *123*, 2672–2679.
(51) Tripathi, B. N.; Bhatt, I.; Dietz, K. J. *Protoplasma* **2009**, *235*, 3–15.
(52) Su, B.; Hatay, I.; Ge, P. Y.; Mendez, M.; Corminboeuf, C.; Samec, Z.; Ersoz, M.; Girault, H. H. *Chem. Commun. (Cambridge, U. K.)* **2010**, *46*, 2918–2919.
(53) Larkin, J. D.; Markham, G. D.; Milkevitch, M.; Brooks, B. R.; Bock, C. W. *J. Phys. Chem. A* **2009**, *113*, 11028–11034.
(54) Lu, Q.; Li, X.; Wang, Y.; Chen, G. *J. Mol. Model.* **2009**, *15*, 1397–1405.
(55) Stare, J.; Henson, N. J.; Eckert, J. *J. Chem. Inf. Model.* **2009**, *49*, 833–846.
(56) Surawatanawong, P.; Tye, J. W.; Hall, M. B. *Inorg. Chem.* **2010**, *49*, 188–198.
(57) Bach, R. D.; Dmitrenko, O. *J. Org. Chem.* **2010**, *75*, 3705–3714.
(58) Silaghi-Dumitrescu, R. *J. Porphyrins. Phthalocyanines* **2010**, *14*, 371–374.
(59) Alfonso-Prieto, M.; Biarnés, X.; Vidossich, P.; Rovira, C. *J. Am. Chem. Soc.* **2009**, *131*, 11751–11761.
(60) Srnec, M.; Aquilante, F.; Ryde, U.; Rulísek, L. *J. Phys. Chem. B.* **2009**, *113*, 6074–6086.
(61) Zampella, G.; Fantucci, P.; Pecoraro, V. L.; De Gioia, L. *Inorg. Chem.* **2006**, *45*, 7133–43.
(62) Moreno, J.; David, M.; Roman, T.; Sakaue, M.; Kasai, H. *Extended Abstracts of the 2010 International Conference on Solid State Devices and Materials*; The Japan Society of Applied Physics: Tokyo, 2010; pp 583−584.
(63) Balbuena, P. B.; Calvo, S. R.; Lamas, E. J.; Salazar, P. F.; Seminario, J. M. *J Phys Chem B.* **2006**, *110*, 17452–17459.
(64) Nori-Shargh, D.; Yahyaei, H.; Boggs, J. E. *J. Mol. Graph. Model.* **2010**, *28*, 807–813.
(65) Lukacova, V.; Peng, M.; Fanucci, G.; Tandlich, R.; Hinderliter, A.; Maity, B.; Manivannan, E.; Cook, G. R.; Balaz, S. *J. Biomol. Screen.* **2007**, *12*, 186–202.
(66) Pohle, W.; Gauger, D. R.; Bohl, M.; Mrazkova, E.; Hobza, P. *Biopolymers.* **2004**, *74*, 27–31.
(67) Mulkidjanian, A. Y.; Heberle, J.; Cherepanov, D. A. *Biochim. Biophys. Acta* **2006**, *1757*, 913–930.
(68) Haro, M.; Giner, B.; Lafuente, C.; López, M. C.; Royo, F. M.; Cea, P. *Langmuir.* **2005**, *21*, 2796–2803.
(69) Adelroth, P.; Brzezinski, P. *Biochim. Biophys. Acta* **2004**, *1655*, 102–115.
(70) Squadrito, G. L.; Postlethwait, E. M.; Matalon, S. *Am. J. Physiol.: Lung Cell. Mol. Physiol.* **2010**, *299*, L289–300.
(71) Zamora, R.; Hidalgo, F. J. *Chem. Res. Toxicol.* **2003**, *16*, 1632–1641.
(72) Wachtel, E.; Bach, D.; Epand, R. F.; Tishbee, A.; Epand, R. M. *Biochemistry* **2006**, *45*, 1345–1351.
(73) Gabriel, B.; Prats, M.; Teissié, J. *Biochemistry* **1991**, *30*, 9359–9364.
(74) Teissié, J.; Gabriel, B.; Prats, M. *Trends Biochem. Sci.* **1993**, *18*, 243–246.
(75) Suits, F.; Pitman, M. C.; Feller, S. E. *J. Chem. Phys.* **2005**, *122*, 244714.
(76) Murzyn, K.; Róg, T.; Pasenkiewicz-Gierula, M. *Biophys. J.* **2005**, *88*, 1091–1103 .
(77) Delley, B. *Mol. Simul.* **2006**, *32*, 117–123 .
(78) Klamt, A.; Schüürmann, G. *J. Chem. Soc., Perkin Trans. 2* **1993**, 799–805.
(79) Andzelm, J.; Kölmel, C.; Klamt, A. *J. Chem. Phys.* **1995**, *103*, 9312–9320.
(80) Delley, B. *J. Chem. Phys.* **2000**, *113*, 7756–7764.
(81) Delley, B. *J. Phys. Chem.* **1996**, *100*, 6107–6110.
(82) Delley, B. *J. Chem. Phys.* **1990**, *92*, 508–517.
(83) Perdew, J. P.; Burke, K.; Ernzerhof, M. *Phys. Rev. Lett.* **1996**, *77*, 3865–3868.
(84) Perdew, J. P.; Chevary, J. A.; Vosko, S. H.; Jackson, K. A.; Pederson, M. R.; Singh, D. J.; Fiolhais, C. *Phys. Rev. B: Condens. Matter Mater. Phys.* **1992**, *46*, 6671–6687.
(85) Lee, C. S.; Hwang, T. S.; Wang, Y.; Peng, S. M.; Hwang, C. S. *J. Phys. Chem.* **1996**, *100*, 2934–2941.
(86) Wang, Z. G.; Zeng, Q. D.; Luan, Y. B.; Wu, X. J.; Wan, L. J.; Wang, C.; Lee, G. U.; Yin, S. X.; Yang, J. L.; Bai, C. L. *J. Phys. Chem. B.* **2003**, *107*, 13384–13388.
(87) Lin, T. T.; Zhang, W. D.; Huang, J. C.; He, C. B. *J. Phys. Chem. B.* **2005**, *109*, 13755–13760.
(88) Inada, Y.; Orita, H. *J. Comput. Chem.* **2008**, *29*, 225–232.
(89) Andzelm, J.; Govind, N.; Fitzgerald, G.; Maiti, A. *Int. J. Quantum Chem.* **2003**, *91*, 467–473.
(90) Halgren, T. A.; Lipscomb, W. N. *Chem. Phys. Lett.* **1977**, *49*, 225–232.

(91) Davies, D. M.; Foggo, S. J.; Paradis, P. M. *J. Chem. Soc., Perkin. Trans. 2* **1998**, 1381–1383.
(92) Colodette, J. L.; Rothenberg, S.; Dence, C. *J. Pulp Pap. Sci.* **1989**, *15*, 3–10.
(93) Mussatto, S. I.; Rocha, G. J. M.; Roberto, I. C. *Cellulose.* **2008**, *15*, 641–649.
(94) Ramo, J. *Hydrogen Peroxide-Metals-Chelating Agents: Interactions and Analytical Techniques*; Oulu University Press: Oulu, Finland, 2003; pp 26−28.
(95) Rahmawati, N.; Ohashi, Y.; Honda, Y.; Kuwahara, M.; Fackler, K.; Messner, K.; Watanabe, T. *Chem. Eng. J.* **2005**, *112*, 167–171.
(96) Brooks, R. E.; Moore, S. B. *Cellulose* **2000**, *7*, 263–286.
(97) Seelig, J.; Macdonald, P. M.; Scherer, P. G. *Biochemistry* **1987**, *26*, 7535–7541.
(98) Tobias, D. J. *Curr. Opin. Struct. Biol.* **2001**, *11*, 253–261.
(99) Plesnicar, B.; Cerkovnik, J.; Tekavec, T.; Koller, J. *J. Am. Chem. Soc.* **1998**, *120*, 8005–8006.
(100) Engdahl, A.; Nelander, B. *Science* **2002**, *295*, 482–483.
(101) Nyffeler, P. T.; Boyle, N. A.; Eltepu, L.; Wong, C. H.; Eschenmoser, A.; Lerner, R. A.; Wentworth, P., Jr. *Angew. Chem., Int. Ed.* **2004**, *43*, 4656–4659.
(102) Suma, K.; Sumiyoshi, Y.; Endo, Y. *J. Am. Chem. Soc.* **2005**, *127*, 14998–14999.
(103) Derro, E. L.; Murray, C.; Sechler, T. D.; Lester, M. I. *J. Phys. Chem. A.* **2007**, *111*, 11592–115601.
(104) Kraka, E.; Cremer, D.; Koller, J.; Plesnicar, B. *J. Am. Chem. Soc.* **2002**, *124*, 8462–70.
(105) Zheng, W.; Jewitt, D.; Kaiser, R. I. *Phys. Chem. Chem. Phys.* **2007**, *9*, 2556–2563.
(106) Xu, X.; Goddard, W. A. *Proc. Natl. Acad. Sci. U.S.A.* **2002**, *99*, 15308–15312.
(107) Shukla, P. K.; Mishra, P. C. *J. Phys. Chem. B.* **2007**, *111*, 4603–4615.
(108) Wentworth, P.; Wentworth, A. D.; Zhu, X.; Wilson, I. A.; Janda, K. D.; Eschenmoser, A.; Lerner, R. A. *Proc. Natl. Acad. Sci. U.S.A.* **2003**, *100*, 1490–1493.
(109) Arnau, J. L.; Giguère, P. A. *J. Chem. Phys.* **1974**, *60*, 270–273.
(110) Giguere, P. A.; Srinivasan, T. K. K. *Chem. Phys. Lett.* **1975**, *33*, 479–482.
(111) Datta, D.; Vaidehi, N.; Xu, X.; Goddard, W. A. *Proc. Natl. Acad. Sci. U.S.A.* **2002**, *99*, 2636–2641.
(112) Wentworth, P.; Jones, L. H.; Wentworth, A. D.; Zhu, X.; Larsen, N. A.; Wilson, I. A.; Xu, X.; Goddard, W. A.; Janda, K. D.; Eschenmoser, A.; Lerner, R. A. *Science* **2001**, *293*, 1806–1811.
(113) Serowy, S.; Saparov, S. M.; Antonenko, Y. N.; Kozlovsky, W.; Hagen, V.; Pohl, P. *Biophys. J.* **2003**, *84*, 1031–1037.
(114) Tuttle, T.; Cerkovnik, J.; Koller, J.; Plesnicar, B. *J. Phys. Chem. A.* **2010**, *114*, 8003–8008.
(115) Koller, J.; Plesnicar, B. *J. Am. Chem. Soc.* **1996**, *118*, 2470–2472.
(116) Xu, X.; Muller, R. P.; Goddard, W. A. *Proc. Natl. Acad. Sci. U.S.A.* **2002**, *99*, 3376–3381.
(117) Zhu, X.; Wentworth, P.; Wentworth, A. D.; Eschenmoser, A.; Lerner, R. A.; Wilson, I. A. *Proc. Natl. Acad. Sci. U.S.A.* **2004**, *101*, 2247–2252.
(118) Datta, D.; Vaidehi, N.; Xu, X.; Goddard, W. A. *Proc. Natl. Acad. Sci. USA.* **2002**, *99*, 2636–2641.
(119) Uemi, M.; Ronsein, G. E.; Miyamoto, S.; Medeiros, M. H.; Di Mascio, P. *Chem. Res. Toxicol.* **2009**, *22*, 875–884.
(120) Cerkovnik, J.; Tuttle, T.; Kraka, E.; Lendero, N.; Plesnicar, B.; Cremer, D. *J. Am. Chem. Soc.* **2006**, *128*, 4090–4100.
(121) Plesnicar, B.; Tuttle, T.; Cerkovnik, J.; Koller, J.; Cremer, D. *J. Am. Chem. Soc.* **2003**, *125*, 11553–11564.
(122) Plesnicar, B.; Cerkovnik, J.; Tekavec, T.; Koller, J. *Chemistry* **2000**, *6*, 809–819.
(123) Mckay, D. J.; Wright, J. S. *J. Am. Chem. Soc.* **1998**, *120*, 1003–1013.
(124) Kovacic, S.; Koller, J.; Cerkovnik, J.; Tuttle, T.; Plesnicar, B. *J. Phys. Chem. A.* **2008**, *112*, 8129–8135.